Supplement of Atmos. Chem. Phys., 26, 3589–3606, 2026
https://doi.org/10.5194/acp-26-3589-2026-supplement
© Author(s) 2026. CC BY 4.0 License.

Atmospheric Chemistry and Physics
Open Access
EGU

Supplement of

Degradation of anhydro-saccharides and the driving factors in real atmospheric conditions: a cross-city study in China

Biao Zhou et al.

Correspondence to: Li Li (lily@shu.edu.cn) and Jian Zhen Yu (jian.yu@ust.hk)

The copyright of individual parts of the supplement might differ from the article licence.

Texts

Tables

Figures

temperature in (a) Changzhou, (b) Zibo and (c) Hong Kong

Fig. S5 Correlation of decay rates between levoglucosan, mannosan and galactosan in (a) Zibo, (b) Changzhou and (c) Hong Kong

Fig. S6 Results of residual tests for GAM on the diurnal decay rate of levoglucosan: (a) residual Q-Q plot; (b) scatter plot of residuals vs. predicted values; (c) histogram of residuals; (d) scatter plot of observed values vs. predicted values

S1. Standard preparation

We used the stock solution for dilution to make the standards, which is all purchased from Anple. The working standard solution was freshly prepared by diluting stock solutions several times using 10 mL flasks, respectively with acetonitrile (ACN) and dichloromethane (DCM) solvent, producing final working solution concentrations are shown in Table S2. Table S2 shows the corresponding IS and other details for external standards (ESs). Table S3 lists the standard preparation details for internal standards.

Different volumes ranging from 5 to 25 μL of working standard solution and a fixed volume (5 μL) of ISs were injected into the collection and thermal desorption cell (CTD) to build calibration curves using the same analysis procedure as that for the samples. Calibration curves were constructed by fitting the normalized peak area of ESs to their corresponding ISs.

S2. Derivation of a decay rate using an inert substance as the reference

The rate expression for the concentration of species *i* in the atmosphere can be written as (Donahue et al., 2005):

$$\frac{\partial C_i}{\partial t} = -k_{ri} \cdot C_{OX} \cdot (1 + f_i) - k_{d_i} \cdot C_i - k_{d'_i} \cdot C_i + E_i \quad \text{(S1)}$$

$$f_i = < \frac{C'_{ox} \cdot C'_i}{C_{OX} \cdot C_i} \quad \text{(S2)}$$

k_{ri} is the second-order reaction rate constant of species *i* in the aerosol, C_i is the measured concentration of species *i* in the aerosol, C_{OX} is the average oxidant concentration in the aerosol, k_{d_i} and $k_{d'_i}$ are the dilution and deposition rate constant of the species *i*, E_i is the source emission rate of species *i*, f_i is a fractional covariance term that describes spatial variations of the reactants within the particle. f_i is zero if either oxidant or the reactant species *i* is well mixed (i.e., gradients $C'_{ox} = 0$ or $C'_i = 0$). f_i is greater than zero when species *i* and oxidant are concentrated

at the particle surface. f_i is negative when species *i* is depleted near the particle surface and the oxidant is concentrated near the particle surface(Huff Hartz et al., 2007).

The interference from source emissions, atmospheric dilution and deposition can be eliminated by using the concentration ratio of $\frac{C_i}{C_j}$, that is, species *i* is normalized by a reference species *j* which showed the same source origins, thus:

$$\frac{\partial \frac{C_i}{C_j}}{\partial t} = -\left\{k_{r_i} \cdot C_{OX} \cdot (1 + f_i) - k_{r_j} \cdot C_{OX} \cdot (1 + f_j)\right\} \cdot \frac{C_i}{C_j} - \left(k_{d_i} - k_{d_j}\right) \cdot \frac{C_i}{C_j} - \left(k_{d'_i} - k_{d'_j}\right) \cdot \frac{C_i}{C_j} + \left(E_i - E_j\right) \quad \text{(S3)}$$

Assuming the deposition and dilution rate and fractional covariance term for species i and j are not species dependent, i.e., $k_{d_i} = k_{d_j}$, $k_{d'_i} = k_{d'_j}$, $f_i = f_j$. In our consideration, the species i and j are from the same source. If they show comparable emission rates, i.e., $E_i \cong E_j$, or there are no fresh emissions or emissions are negligible within the consideration timeframe, i.e., $E_i \cong 0$ and $E_j \cong 0$, then:

$$\frac{\partial \frac{C_i}{C_j}}{\partial t} = -\left(k_{ri} - k_{rj}\right) \cdot (1 + f_i) \cdot C_{OX} \cdot \frac{C_i}{C_j} \quad \text{(S4)}$$

If we consider a scenario where the reaction occurs at or near the aerosol surface, the reagent concentration within the particle is well mixed initially, thus $f_i = 0$ and the following equation holds:

$$\frac{\partial \frac{C_i}{C_j}}{\partial t} = -(k_{ri} - k_{rj}) \cdot C_{OX} \cdot \frac{C_i}{C_j} \quad \text{(S5)}$$

Applying the identity $\frac{\partial\, ln(x)}{\partial t} = (\frac{\partial x}{\partial t}) \cdot (\frac{1}{x})$, and Equation 5 can be rewritten as：

$$\frac{\partial\, ln(C_i/C_j)}{\partial t} = -(k_{ri} - k_{rj}) \cdot C_{OX} \quad \text{(S6)}$$

To determine the decay rate of the BB-emitted saccharides, we select the K^+_{BB} as the reference species j. K^+_{BB} is inert to the oxidants ($k_{rj} = 0$), thus:

$$\frac{\partial\, ln(C_i/C_{K^+_{BB}})}{\partial t} = -k,\ k = k_{ri} \cdot C_{OX} \quad \text{(S7)}$$

Table S1 Online instruments and analysis methods of meteorological parameters, conventional pollutants, as well as $PM_{2.5}$-bound OC/EC and inorganic compounds

Instrument	Machine type	Manufacturer	Monitoring factors	Analytical Principle
Zibo, Shandong province, NCP				
$PM_{2.5}$ online monitor	MODEL 5014i	Thermo Fisher Scientific, US	$PM_{2.5}$	Beta-ray method
NO_x analyzer	MODEL 42i	Thermo Fisher Scientific, US	NO、NO_2、NO_x	Pulsed fluorescence method
Ozone Analyzer	MODEL 49i	Thermo Fisher Scientific, US	O_3	Differential absorption spectroscopy
Aerosol compositions monitor	MODEL S611	Fortelice International Co., Ltd., Taiwan, China	Cl^-、NO_3^-、SO_4^{2-}、Na^+、NH_4^+、K^+、Mg^{2+}、Ca^{2+}、NH_3	Ion chromatography
OC/EC online monitor	MODEL ECOC-610	Hangzhou Pengpu Technology Co., Ltd., China	OC、EC	Thermal light Method
Meteorological monitor	\	China Meteorological Administration	WS、WD、RH、T、P、RF	https://www.cma.gov.cn/
Solar radiation analyzer	CMP11	Kipp & Zonen, Zuid-Holland, Netherlands	SSR	Pulsed light signal method
Changzhou, Jiangsu province, YRD				
Meteorological monitor	WXT520	VAISALA, FL	WS、WD、RH、T、P、RF	Ultrasonic and capacitive measurement methods
$PM_{2.5}$ online monitor	BAM1020	Met One, US	$PM_{2.5}$	Beta-ray method
Ozone Analyzer	MODEL 49i	Thermo Fisher Scientific, US	O_3	Differential absorption spectroscopy
NO_x analyzer	MODEL42i	Thermo Fisher Scientific, US	NO、NO_2、NO_x	Pulsed fluorescence method
OC/EC online monitor	RT-4	Sunset Laboratory, US	OC、EC	Thermal light Method
MARGA ionic online analyzer	ADI2080	Metrohm, CHN	Cl^-、NO_3^-、SO_4^{2-}、Na^+、NH_4^+、K^+、Mg^{2+}、Ca^{2+}、NH_3	Ion chromatography
HongKong, PRD				
MARGA ionic online analyzer	ADI2080	Metrohm, CHN	Cl^-、NO_3^-、SO_4^{2-}、Na^+、NH_4^+、K^+、Mg^{2+}、Ca^{2+}、NH_3	Ion chromatography
OC/EC online monitor	RT-4	Sunset Laboratory, US	OC、EC	Thermal light Method
$PM_{2.5}$ online monitor	Model 5030i	Thermo Fisher Scientific, US	$PM_{2.5}$	Beta-ray method

Ozone Analyzer	MODEL 49i	Thermo Fisher Scientific, US	O_3	Differential absorption spectroscopy
NO_x analyzer	MODEL42i	Thermo Fisher Scientific, US	NO、NO_2、NO_x	Pulsed fluorescence method
Gas pollutants analyzer	AWS tower	Hong Kong Environment Protection Department	WS、WD、RH、T、P、RF 、O_3、SSR、SO_2、NO、NO_2、NO_x	\
elemental species analyzer	Xact 625i	Cooper Environmental Services	K、Ca	X-ray method

Table S2 A list of corresponding internal standard (IS) and other details for external standards (ESs) and compounds identified in samples

Compound	Formula	Solvent	Quantification IS	Working solution (ng/μL).	Quantification ion
Levoglucosan	C6H10O5	DCM + ACN	Levoglucosan-d_7	0.294	204
Galactosan	C6H10O5			0.293	217
Mannosan	C6H10O5			0.294	204

Table S3 A list of standard preparation details for internal standard (IS) deployed during the campaign

Compound	Formula	Solvent	Working solution (ng/μL)	Quantification ion
Levoglucosan-d_7	C6H3D7O5	DCM + ACN	1.046	206

Table S4 Statistical summary of meteorological conditions, average ± standard deviation of hourly concentrations of conventional atmospheric pollutants and TAG-determined anhydro-saccharides during the field campaign

Measurement parameters	ZB	CZ	HK
$PM_{2.5}$ (μg/m³)	69.4±58.0	49.9±26.4	20.5±8.8
T (℃)	-0.2±6.1	10.9±4.9	19.6±5.2
RH (%)	52.1±22.3	56.6±18.4	68.4±17.51
NO_2 (μg/m³)	44.4±24.6	45.2±24.8	5.8±6.6
O_3 (μg/m³)	59.2±16.2	68.9±26.7	56.9±12.2
WS (m/s)	2.2±1.7	1.3±0.7	3.3±1.7
SO_4^{2-} (μg/m³)	8.8±7.3	6.3±2.7	9.4±8.3
NO_3^- (μg/m³)	15.0±15.2	17.6±11.7	2.5±2.6
OC (μg/m³)	7.7±4.9	6.0±3.7	3.6±2.0
EC (μg/m³)	3.3±2.4	1.9±1.4	1.2±0.8
Levoglucosan (ng/m³)	45.5 ± 32.3	45.1±38.7	27.6±15.6
Mannosan (ng/m³)	2.4±1.7	3.6±3.2	1.9±1.5
Galactosan (ng/m³)	4.5±3.4	2.4±2.0	0.9±0.7

Table S5 Daytime decay rates of anhydro-saccharides at the three sites calculated using the relative rate constant method

Decay of anhydro-saccharides	ZB	CZ	HK
k_lev	0.103±0.027	0.126±0.052	0.097±0.011
k_man	0.095±0.033	0.128±0.070	0.137±0.015
k_gal	0.105±0.034	0.133±0.082	0.147±0.016

Table S6 Results of GAM analysis

Smooth variables	Edf	Ref.df	F	*p*
ALWC	1.0	9.0	5.2	0.02
T	2.5	9.0	8.7	0.001
O_x	1.8	9.0	6.5	0.01
RH	3.2	9.0	3.1	0.08
SSR	4.0	9.0	2.3	0.12
Deviance explained (%) = 65.8%				
R^2=0.66				

Table S7 Variance inflation factors (VIF) of the influencing factors for the decay rate of anhydro-saccharides in GAM analysis

Smooth variables	ALWC	T	O_x	RH	SSR
k_lev	1.3	1.5	1.4	1.5	1.6
k_man	1.3	1.5	1.4	1.5	1.6
k_gal	1.3	1.5	1.4	1.5	1.6

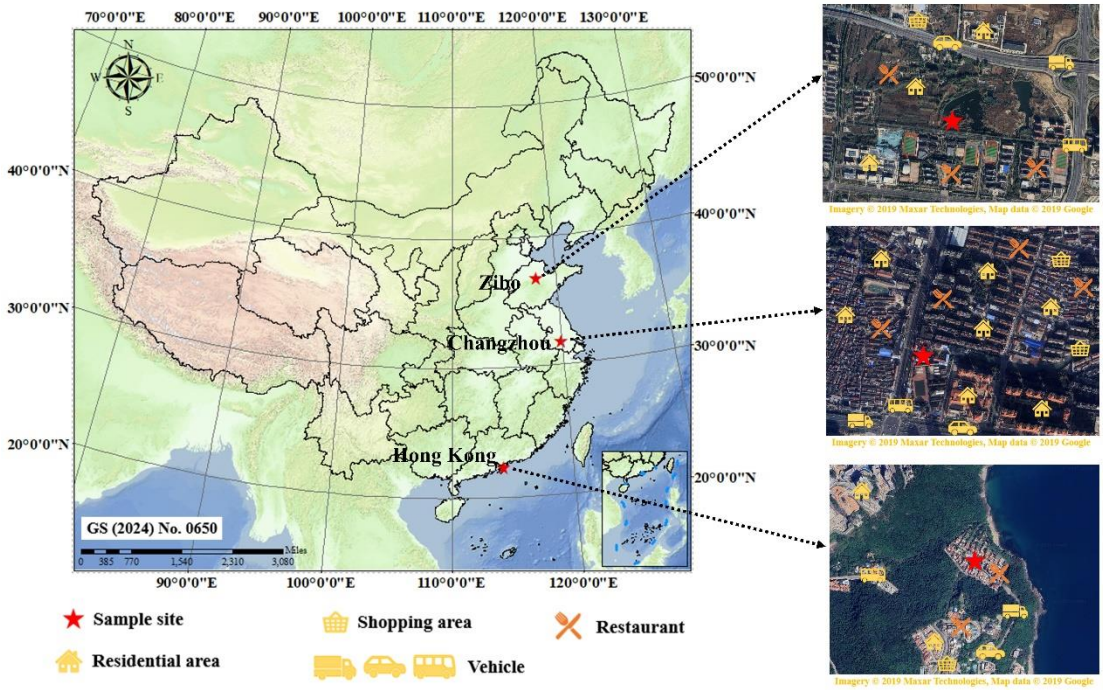

Fig. S1 Locations of the sampling sites (The three satellite inset maps show the distribution of residential areas, shopping areas, restaurants, and vehicles in the immediate vicinity of each sampling site.)

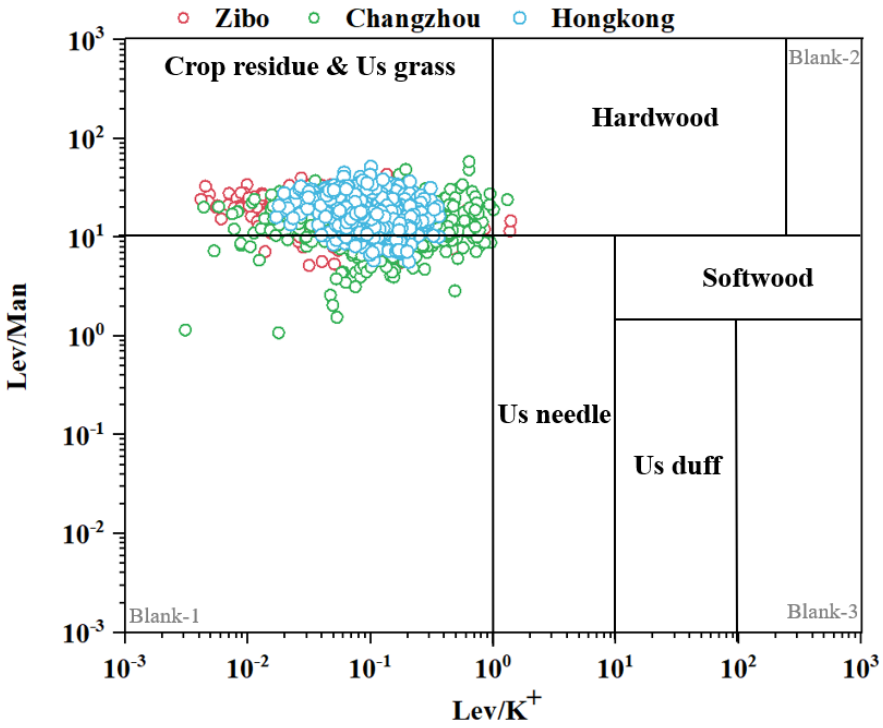

Fig. S2 Distribution of levoglucosan/K^+ ratios and levoglucosan/mannosan ratios from ambient measurement, with the corresponding ratios for different kinds of biomass burning types from Cheng et al. (2013) (Note that K_{BB} at the Hong Kong site is used as a substitute for K^+, with further details available in Wang et al., 2025.)

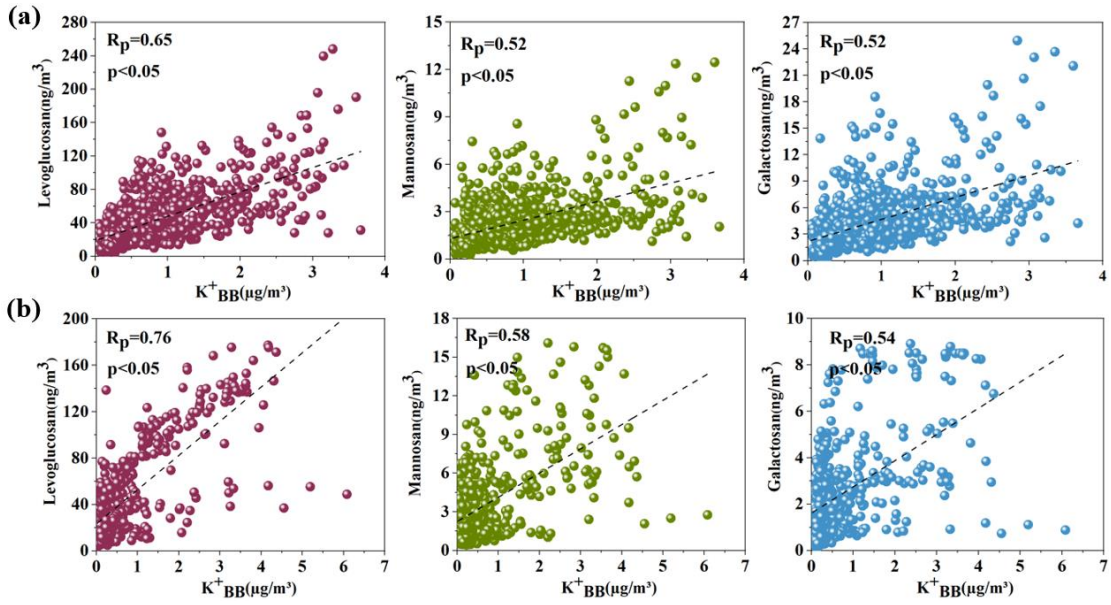

Fig. S3 Scatter plots showing the correlation of levoglucosan, mannosan, and galactosan as a function of K^+_{BB} in (a) Zibo and (b) Changzhou

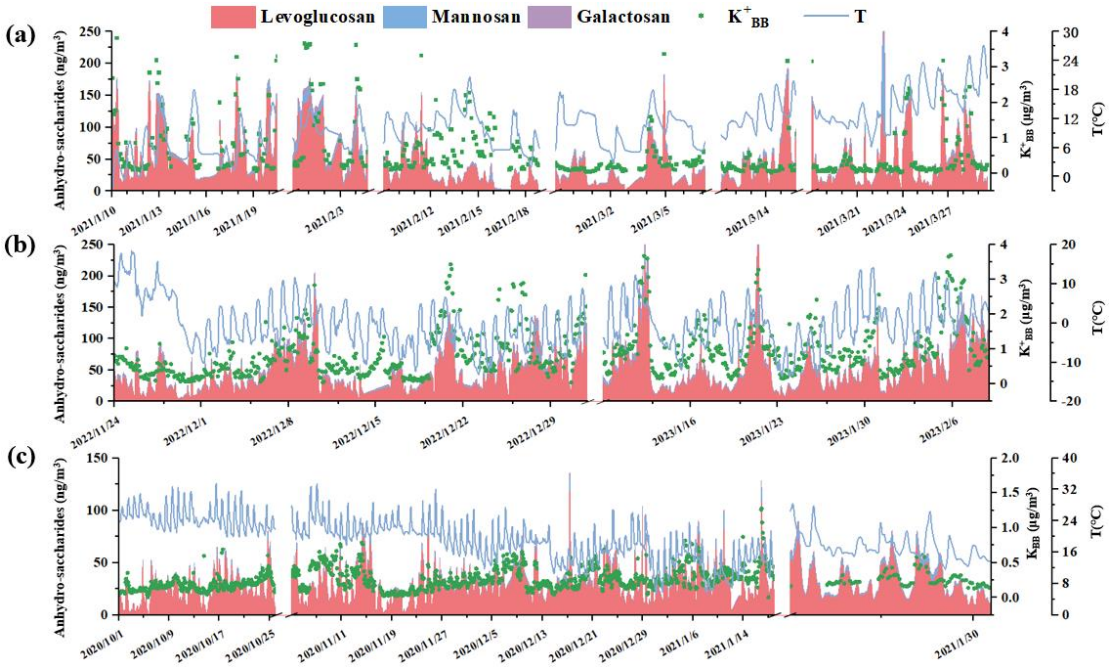

Fig. S4 Time series of concentrations of levoglucosan, mannosan, galactosan and K^+_{BB}, as well as temperature in (a) Changzhou, (b) Zibo and (c) Hong Kong

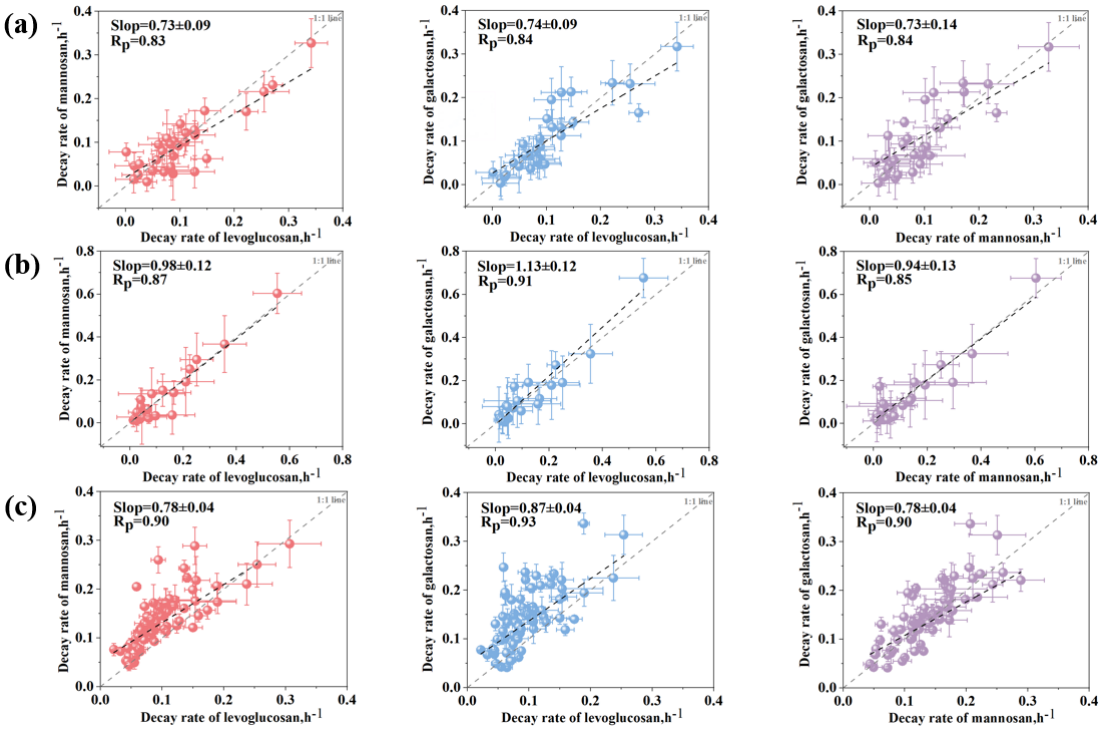

Fig. S5 Correlation of decay rates between levoglucosan, mannosan and galactosan in (a) Zibo, (b) Changzhou and (c) Hong Kong

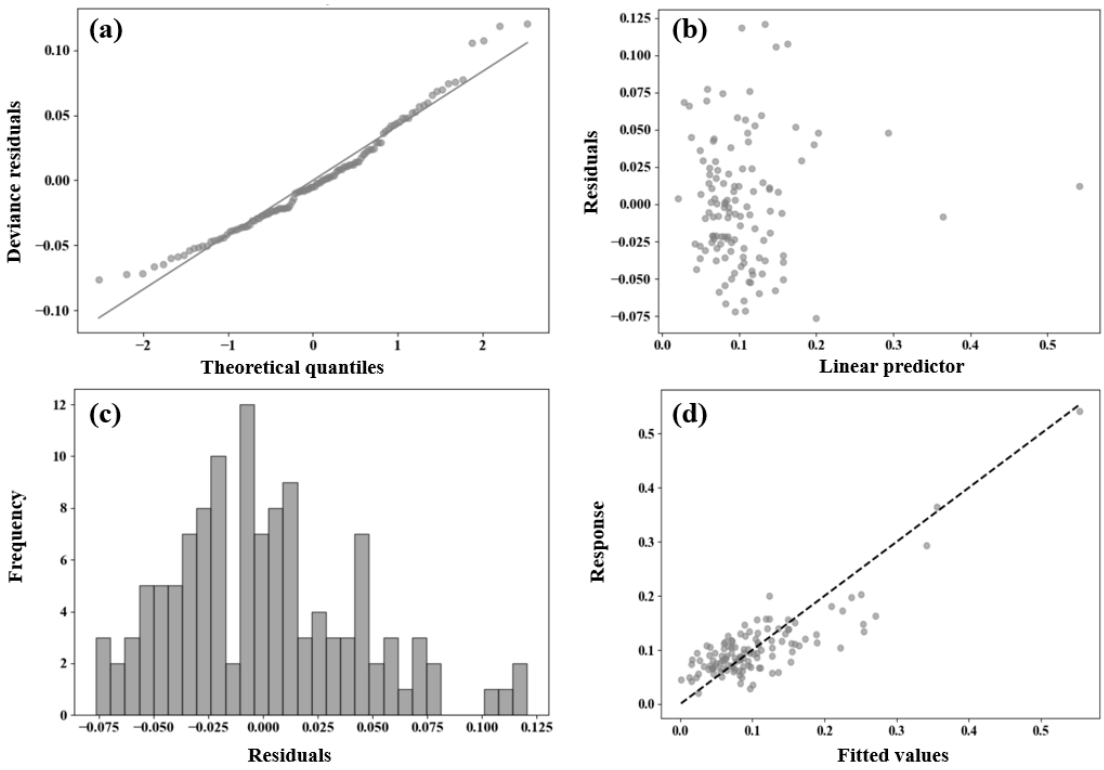

Fig. S6 Results of residual tests for GAM on the diurnal decay rate of levoglucosan: (a) residual Q-Q plot; (b) scatter plot of residuals vs. predicted values; (c) histogram of residuals; (d) scatter plot of observed values vs. predicted values

References

Donahue, N.M., Robinson, A.L., Hartz, K.E.H., Sage, A.M., and Weitkamp, E.A.: Competitive oxidation in atmospheric aerosols: The case for relative kinetics, Geophys. Res. Lett., 32, http://dx.doi.org/10.1029/2005gl022893, 2005.

Huff Hartz, K.E., Weitkamp, E.A., Sage, A.M., Donahue, N.M., and Robinson, A.L.: Laboratory measurements of the oxidation kinetics of organic aerosol mixtures using a relative rate constants approach, J. Geophys. Res.:Atmos., 112, http://dx.doi.org/10.1029/2006jd007526, 2007.

Li, Q., Zhang, K., Li, R., Yang, L., Yi, Y., Liu, Z., Zhang, X., Feng, J., Wang, Q., Wang, W., Huang, L., Wang, Y., Wang, S., Chen, H., Chan, A., Latif, M.T., Ooi, M.C.G., Manomaiphiboon, K., Yu, J., and Li, L.: Underestimation of biomass burning contribution to $PM_{2.5}$ due to its chemical degradation based on hourly measurements of organic tracers: A case study in the Yangtze River Delta (YRD) region, China, Sci. Total Environ., 872, http://dx.doi.org/10.1016/j.scitotenv.2023.162071, 2023.

Wang, Q., Wang, S., Chen, H., Zhang, Z., Yu, H., Chan, M.N., and Yu, J.Z.: Ambient Measurements of Daytime Decay Rates of Levoglucosan, Mannosan, and Galactosan, J. Geophys. Res.:Atmos., 130, http://dx.doi.org/10.1029/2024jd042423, 2025.

Wang, Q. and Yu, J.Z.: Ambient Measurements of Heterogeneous Ozone Oxidation Rates of Oleic, Elaidic, and Linoleic Acid Using a Relative Rate Constant Approach in an Urban Environment, Geophys. Res. Lett., 48, http://dx.doi.org/10.1029/2021gl095130, 2021.

Williams, B.J., Goldstein, A.H., Kreisberg, N.M., and Hering, S.V.: An In-Situ Instrument for Speciated Organic Composition of Atmospheric Aerosols: Thermal Desorption Aerosol GC/MS-FID (TAG). Aerosol. Sci. Technol. 40, 627-638. http://dx.doi.org/10.1080/02786820600754631, 2006.